scientific reports

Check for updates

OPEN

Elevational microhabitats influence some endolichenic traits of *Umbilicaria aprina*, an alpine lichen species

Marziye Rahimi-Rizi[1], Hooman Norouzi[2]✉, Mohammad Sohrabi[3], Samaneh Dashtipoor[4], Mitra Omidi Nasab[4] & Joel Boustie[5]

Understanding the dynamics of lichen-environment interactions, particularly in terms of elemental composition, microbial, and metabolic profiles, is crucial for elucidating the adaptive strategies of lichens. Here we aimed to investigate the impact of elevational microhabitats on the elemental compositions, microbial profiles, and metabolic profiles of different colonies of *Umbilicaria aprina* along an elevational gradient. Ionomics showed variations in elemental compositions of colonies at different elevations with distinct patterns of accumulation for specific elements. Untargeted metabolomics revealed metabolic alterations in different colonies of *U. aprina* across elevations, suggesting a potential role of lichen secondary metabolites in responding to environmental changes. Culture-based analysis of microbiome also showed variations in the microbial profiles of colonies with changes in elevation, confirming the influence of elevational microhabitats on lichen-associated microbial communities. We further examined possible correlations between the relative intensity of different metabolites and the other two endolichenic traits (i.e., elemental composition and microbial profile). Although no consistent correlative patterns emerged, some metabolite-specific correlations were observed. Overall, our study shows that certain endolichenic traits undergo variations even within a restricted alpine range, corresponding to minor changes in environmental conditions.

Keywords *Umbilicaria aprina*, Untargeted metabolomics, Endolichenic fungi, Lichen-associated bacteria, Elemental composition, Elevational microhabitats

Lichen is a self-sustaining community consisting of a primary mycobiont, a morphologically undifferentiated alga, and potentially a cyanobacterium as the primary (or secondary) photobiont, along with an obligatory microbial community comprising yeasts and bacteria[1]. This symbiotic association, akin to a greenhouse, is inherently susceptible to environmental changes. Within this sessile association, each partner perceives and responds to environmental factors. For instance, the mycobiont primarily responds to environmental signals through discernible chemical fluctuations[2–6]. Various environmental factors have been reported to influence the physiological processes and chemical status of lichens. These factors include, but are not limited to, altitude[7], temperature[8–10], moisture, irradiance[11–15], slope aspect[16], season[17], and precipitation[18]. The microbial communities within lichen thalli can also be altered by biotic and abiotic factors[19]. Age, irradiance, substrate[20,21], climate warming[22], and microclimatic gradients within the lichen thallus[23] are among the contributing factors. Importantly, lichens have been found to exhibit genomic-level responses to environmental changes, which are believed to contribute to the evolution and environmental adaptation of lichen species[24]. Additionally, evidence suggests the involvement of other members of the lichen association in the biosynthesis of lichen substances. For example, Spribille et al.[25] hypothesized that basidiomycete yeasts may be responsible for the biosynthesis of vulpinic acid in certain *Bryoria* species. Other studies highlight the role of the lichen microbiome in various functions, including nutrient and element uptake and supply, as well as resistance against abiotic and biotic stressors[26]. Accordingly, it is plausible to consider the potential involvement of lichen microbial communities in

[1]Department of Horticultural Sciences, Faculty of Agriculture, Bu-Ali Sina University, Hamedan, Iran. [2]Department of Botany, University of Innsbruck, Sternwartestraße 15, 6020 Innsbruck, Austria. [3]The Museum of Iranian Lichens, Iranian Research Organization for Science and Technology, Tehran, Iran. [4]Department of Plant Protection, Faculty of Agriculture, Bu-Ali Sina University, Hamedan, Iran. [5]CNRS, ISCR (Institut des Sciences Chimiques de Rennes) -UMR6226, Univ Rennes, 35000 Rennes, France. ✉email: Hooman.Norouzi@uibk.ac.at

the production of their distinctive secondary metabolites. In other words, if the microbial profile of a particular lichen species changes along an altitudinal gradient, it may lead to concomitant alterations in the metabolic profile of that species.

Most studies on lichens have primarily focused on investigating metabolic and physiological variations across vast geographic regions[9,14,17,27]. Here we aimed to explore the chemical variations of a specific lichen species, *Umbilicaria aprina*, within a limited alpine zone along an altitudinal gradient. Along such a gradient, climatic and biotic factors undergo gradual changes, resulting in distinct microsites. Each microsite exhibits discernibly different combinations of climatic and biotic factors compared to others. Notable factors that may contribute to these changes include, but are not limited to, altitude, precipitation type and amount, temperature, irradiance, slope aspect, and substrate composition. Consequently, our study investigates the potential impacts of microclimatic variations on some endolichenic traits of *Umbilicaria aprina*.

Lichen family Umbilicariaceae, found within the order Umbilicariales of the class Lecanoromycetes, consists of diverse lichens. These saxicolous and mostly foliose lichens often feature a prominent umbilicus at the center of the thallus, inspiring the family's name[28]. Well-studied genera in the Umbilicariaceae family include *Umbilicaria* and *Lasallia*, (MycoBank: https://www.mycobank.org/). Umbilicariaceae species are predominantly found in higher latitude or altitude regions. These species typically produce simple orcinol compounds, including depsides, tridepsides, and β-orcinol depsidones, synthesized via the acetyl-polymalonyl pathway[29]. *U. aprina*, a member of the Umbilicariaceae family, is a lichenized ascomycete that was originally known from Ethiopia[30]. This species thrives across a wide range of latitudes, longitudes, and altitudes, spanning from Antarctica to the Svalbard archipelago. In Iran, there are 11 distinct species of *Umbilicaria*[31], and *U. aprina* is known from alpine habitats of NW Iran with DNA confirmation which corresponds with Genbank FN186063 and FN185930[32]. Previous investigations have examined chemical variations among different ecotypes of this species using liquid chromatography coupled with electrospray ionization tandem mass spectrometry (LC–ESI–MS/MS)[16]. Given the presence of *U. aprina* in Iran's flora and its extensive distribution, it provides an opportunity for conducting comprehensive studies on this species. However, to date, the impact of microclimatic variations on the endolichenic traits of *U. aprina* remains unexplored.

The objective of the study is to characterize the environmentally-induced shifts in the chemical, elemental, and microbial composition of *Umbilicaria aprina* Nyl., in a limited alpine area. To achieve this, we employed metabolomics, ionomics, and culture-based analysis of the microbiome to address the following research queries:

1. Do the metabolomic status and elemental composition of *U. aprina* change along an elevational gradient?
2. Does the microbial profile of *U. aprina* change along an elevational gradient?
3. Do shifts in the elemental composition and microbial profile of *U. aprina* correlate with alterations in the metabolome?

Materials and methods

Study area and sampling

We performed the sampling along an altitudinal gradient (approximately 2500–3300 m a.s.l.) in southern Hamedan, Iran, with a low human population and low air pollution (Fig. 1). The habitat was a mountain steppe abounded with siliceous rocky outcrops and *Astragalus* spp. and *Achillea* spp. as the primary vegetation. In this region, mean annual precipitation ranges from 363 mm, at the lowest elevation, to 526 mm, at the highest elevation. The annual temperature also ranges from 8 to 4 °C along the gradient.

Based on an altitudinal gradient, we chose five sampling sites with elevational intervals of 200 m. All sites were primarily north-facing, and each of them was positioned using GPS. At each site, five separate colonies of *U. aprina* were collected from the surface of siliceous rocks. We chose surfaces that were mainly north-facing to reduce the impact of radiation difference. We also collected thalli of comparable size to minimize the possible differences due to age. The occurrence of the target lichen species at the highest elevation (3350 m a.s.l.) was significantly reduced compared to lower altitudes. Despite rigorous sampling efforts, only four colonies met the criteria for inclusion. One additional colony yielded sufficient biomass solely for culture-based microbial profiling, precluding its inclusion in metabolomic and ionomic analyses. To maintain methodological consistency, we adhered to the 200-m altitudinal intervals across all sampling locations. Thalli which were to be used for metabolomics and ionomics, were stored in plastic bags and transported to the laboratory for pre-treatment and analytical analysis. Samples were identified, and voucher specimens were deposited at the ICH Lichen Herbarium of Iranian Research Organization for Science and Technology (IROST) (Voucher No. 18737). Air-dried samples were reduced to fine powder using a pestle and mortar under a small volume of liquid nitrogen, stored in well-sealed tubes, and kept at room temperature. The samples for microbiome analysis were kept at − 20 °C after collection until they were transported to laboratory, where they were also kept at − 20 °C until analysis.

Reagents

Commercial chemicals and reagents, including analytical acetone, LC–MS grade water, LC–MS grade acetonitrile, dimethyl sulfoxide (DMSO), and formic acid were purchased from Merck (Germany).

Metabolomics

LC–MS/MS analysis

Lichen powder (0.15 g) was defatted twice using *n*-hexane and then extracted in methanol (1.5 ml, 80%). The mixture was then sonicated (40 min at 40 °C). It was afterward centrifuged (9000 rpm for 5 min), and the supernatant was then concentrated in vacuo at 45 °C. Dry extracts were kept at − 20 °C until analysis.

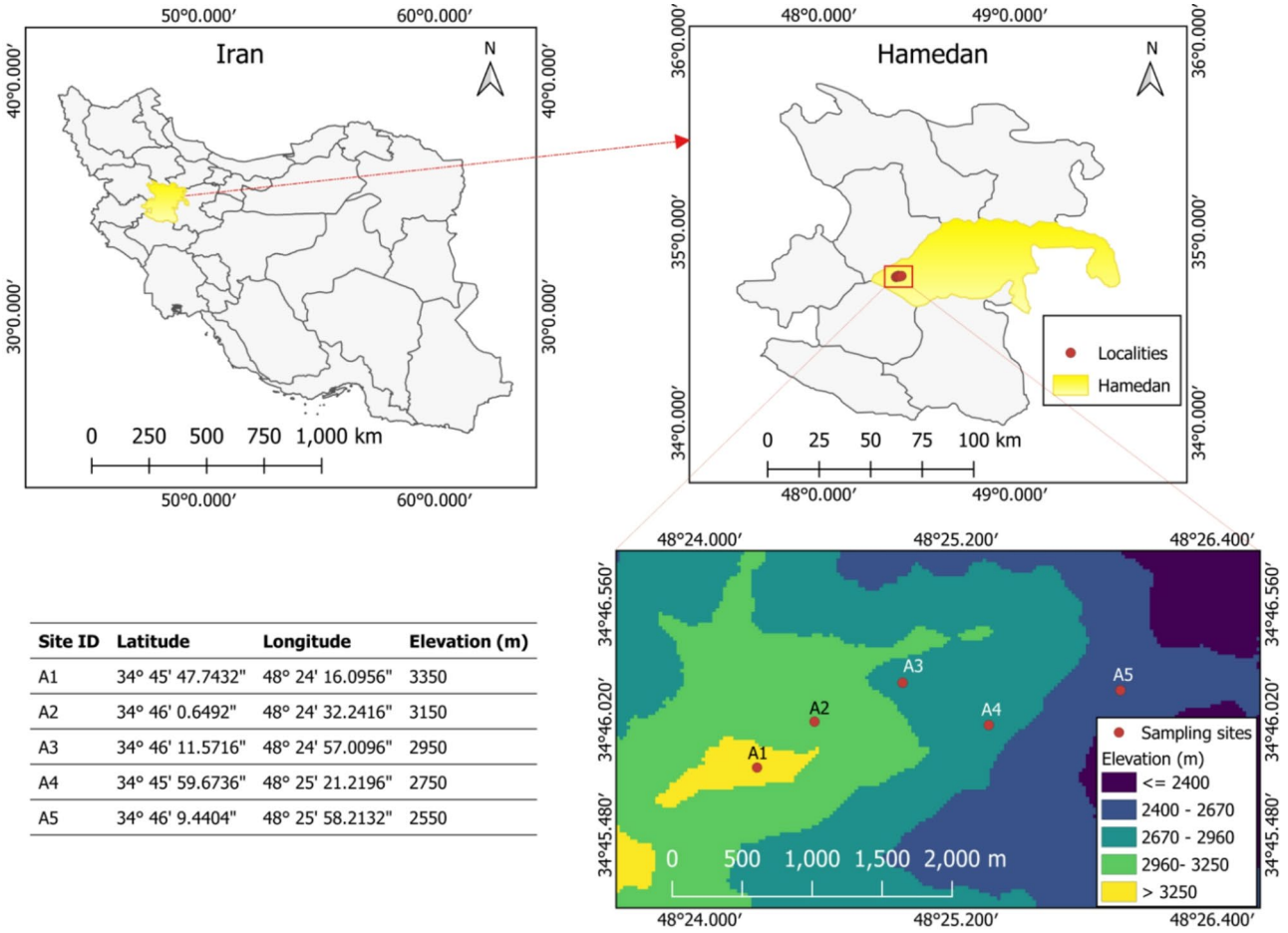

Site ID	Latitude	Longitude	Elevation (m)
A1	34° 45' 47.7432"	48° 24' 16.0956"	3350
A2	34° 46' 0.6492"	48° 24' 32.2416"	3150
A3	34° 46' 11.5716"	48° 24' 57.0096"	2950
A4	34° 45' 59.6736"	48° 25' 21.2196"	2750
A5	34° 46' 9.4404"	48° 25' 58.2132"	2550

Fig. 1. Spatial distribution of five *U. aprina* colonies sampled on Mount Alvand, Hamedan, Iran.

The extracts were re-dissolved in methanol and syringe-filtered (PTFE membrane filters, 0.45 µm, Simplepure, China). 10 µL of each sample was injected into a Waters Alliance e2695 separation module (Milford, MA, USA), and the separation of metabolites was carried out on an Atlantis T3 C18 column (2.1 mm × 100 mm, 3 µm; Milford, MA, USA), whose temperature was set at 30 °C. The separation gradient was a 25-min elution program: 95% A (water + 0.1% formic acid, v/v), gradually turned to 5% A within 20 min, and continued for 5 min by 95% B (acetonitrile). The eluents flow rate was set at 0.25 ml min^{-1}.

The MS/MS analysis was conducted on a Quattro micro-API mass spectrometer (Milford, MA, USA), equipped with an ESI source, in negative ionization mode. The MS parameters were applied as source temperature, 120 ℃; desolvation temperature, 300 °C; Capillary voltage, 3.5 kV; cone voltage, 30 V; collision energy, 30 eV; N2 was used for both nebulizing and drying the gas; mass range, 50–1000 m/*z*. Data acquisition and visualization were performed using MassLynx 4.1.

Raw data pretreatment and multivariate data analysis

Waters raw data (.raw) were converted to mzml format using MSConvert (ProteoWizard 3.0.2). Data pretreatment, including peak detection, chromatogram building, chromatogram deconvolution, isotope grouping, feature alignment, MS row filtering, isotope filtering, gap filling, and normalization, was carried out using MZmine 2.53. A completed feature list was then used for multivariate data analysis using MetaboAnalyst 5.0 (http://www.metaboanalyst.ca/). Principal component analysis (PCA) and partial least squares discriminant analysis (PLS-DA) were performed to compare the samples from different microsites. The variable importance in the projection (VIP) value was used for the tentative evaluation of significantly different metabolites identified with LC–MS/MS (at VIP > 1.0, $p < 0.05$). The metabolites were tentatively identified by comparing their retention time, molecular weight, and MS2 fragment patterns with published references and GNPS (Global Natural Products Social Molecular Networking) Spectral Libraries (https://gnps.ucsd.edu/).

Ionomics

Sample washing and preparation were carried out following Boonpeng et al.[33]. Approximately 100 mg of each sample was accurately weighed into a PTFE digestion vessel, and 5 mL of HNO_3 + HCl (3 + 2 v/v) was added and then maintained for 24 h. The microwave conditions for the sample mineralization were the following: 5 min at 300 W and 20 min at 600 W. The digestion solution was cooled down to room temperature, transferred to a

50 mL volumetric flask, and diluted with ultrapure water to 15 mL. The mineral element content of samples was determined by 7500 Inductively Coupled Plasma Mass Spectrometry (Agilent Technologies, Santa Clara, CA) based on previous methods. A total of 67 mineral elements were targeted, from which only 33 elements could be detected in our samples. Undetected elements likely fell below instrument detection limits or were naturally absent in samples. The operating conditions of the ICP-MS were as follows: RF generator power: 1200 W; RF resonance frequency: 24 MHz; Plasma, auxiliary, and nebulizer gas: argon; Plasma gas flow rate: 12.2 L/min; Auxiliary gas flow rate: 0.8 L/min; Nebulizer gas flow rate: 0.8 L/min; Sample uptake time: 260 S; Measurement replication: 3; Type of detector solid state: CCD; Type of spray chamber cyclonic: modified lichte. The collected data underwent preprocessing using MetaboAnalyst 5.0. Following normalization, we employed principal component analysis (PCA) and partial least squares discriminant analysis (PLS-DA) to compare samples obtained from various microsites. To tentatively assess significantly different elements identified through ICP-MS, we utilized the variable importance in the projection (VIP) values (with a threshold of VIP > 1.0, $p < 0.05$).

Culture-based analysis of the microbiome

Isolation of culturable endolichenic fungi

As shown in Table S1, surface sterilization method was used to obtain endophytes from *U. aprina*[34]. The samples were thoroughly washed with running water to ensure cleanliness. Subsequently, the lichen samples were subjected to sterilization using ethanol and sodium hypochlorite, followed by rinsing with sterile water. The treated samples were then placed on sterile paper. Each lichen sample was carefully cut into small fragments measuring approximately 1 cm. These segments were surface sterilized and subsequently incubated at room temperature for 8 weeks. After the incubation period, individual fungal colonies were isolated by culturing them on a water agar medium in three consecutive rounds. To facilitate further identification, a sterile fine-tipped needle was employed to pick the fungal colonies from the edge and transfer them onto a potato dextrose agar (PDA) medium.

Genomic DNA extraction was performed using a modified CTAB method as described by Möller et al.[35]. In brief, mycelia from the PDA medium were transferred to a 2 ml Eppendorf tube and mixed with 0.5 ml TES buffer. The tube was incubated in hot water for 3 min, followed by cooling on ice for 10 min. Subsequently, proteinase K (2.5 µl) was added, and the tubes were incubated at 65 °C for 30 min. NaCl (5 M, 0.14 ml) and CTAB buffer (10%, 0.65 ml) were added to the mixture, and the tubes were kept in a water bath at 65 °C. After 30 min, a mixture of chloroform and isoamyl alcohol (100 µl, 24:1) was added and briefly mixed. The tubes were then placed on ice for 30 min. Following centrifugation at 12,000 rpm for 10 min, the supernatant was carefully transferred to a new tube and mixed with ammonium acetate (5 M, 225 µl). After a 30-min incubation in cold water, the samples were centrifuged again (12,000 rpm for 10 min). The supernatant was transferred to another tube, and 500 µl of chilled isopropanol was added, followed by centrifugation (12,000 rpm for 10 min). The supernatant was discarded, and the resulting pellets were rinsed twice with 70% ethanol for 1 min, followed by centrifugation (12,000 rpm for 10 min). The pellets were dried and dissolved in TE buffer. The extracted genomic DNA was examined using agarose gel electrophoresis, and satisfactory DNA extracts were further processed for polymerase chain reaction (PCR) and sequencing.

For the amplification of regions of the internal transcribed spacer (ITS) rDNA in fungi, the primers ITS1 (5′-TCCGTAGGTGAACCTGCGG-3′) and ITS4 (5′-TCCTCCGCTTATTGATATGC-3′) were employed. PCR parameters were as follows: 94 °C (3 min), 94 °C (35 cycles, 30 s), 55 °C (40 s), 72 °C (35 s), and 72 °C for 7 min. The amplified products were separated on a 1.5% agarose gel using TAE buffer. The obtained fungal rDNA-ITS sequences were manually edited and compared with sequences available in GenBank databases to facilitate identification. The fungal rDNA-ITS sequences were submitted to the National Center for Biotechnology Information (NCBI), and the accession numbers can be found in Table S1.

Isolation of culturable lichen-associated bacteria

Initially, the samples were washed with sterile distilled water for a duration of 1 min, after which 0.2 g subsamples were excised using sterile scalpels. These subsamples were subsequently surface disinfected by immersing them in 70% ethanol for 1 min, followed by two rinses in sterile distilled water for 5 min each. Next, the subsamples were aseptically fragmented into fine particles and placed in sterile Petri dishes containing a saline solution (0.9% NaCl in distilled water, pH 7.0). To prepare the samples for further analysis, they were subjected to tenfold serial dilutions in sterile phosphate-buffered saline (PBS) solution (10 mM, pH 7.0). The spread plate technique was employed using King's B (KB) medium, a complex non-selective medium supplemented with sterile, filtered cycloheximide (50 mg/l) to inhibit fungal growth. Incubation of the plates was carried out in darkness at 25 °C for 1 week. Morphologically distinct colonies were selected from the same medium for purification, following the protocol described by Biosca et al.[36].

To identify the bacterial isolates, a set of phenotypic and biochemical tests was conducted on the isolated strains, following the methodology outlined by Schaad et al.[37]. The genomic DNA of the bacteria was extracted through enzymatic hydrolysis. Fresh bacteria (50 mg) were added to a 1.5 ml Eppendorf tube, along with 480 µl TE buffer and 20 µl lysozyme solution (2 mg/ml). The bacterial suspension was thoroughly mixed and placed in a shaker for 1 h. Subsequently, the mixture was treated with 50 µl of 20% SDS solution and 5 µl of proteinase K solution, followed by incubation in a water bath at 55 °C for 1 h. DNA extraction was performed twice using the phenol-chloroform-isoamyl alcohol method (25:24:1). The DNA was then precipitated with 80 µl of sodium acetate (3 mol/L, pH 5) and 800 µl of absolute ethanol. After centrifugation at 12,000 rpm for 10 min, the DNA pellet was washed with 70% ethanol and air-dried. The extracted DNA was resuspended in 40 µl of sterile water and stored at − 20 °C for further experiments. The 16S rRNA gene primers, as described by Yeates et al.[38], were employed for PCR amplification of the DNA from each bacterial isolate.

The amplification of the 16S rRNA gene was performed in reaction tubes with a final volume of 25 µl. Each reaction mixture contained 2.5 µl of template DNA, 1 µl of each primer, 12 µl of PCR master mix with standard buffer, and the remaining volume was filled with nuclease-free water. A negative control, consisting of water and PCR reagents without DNA, was included in all PCR experiments. Subsequently, the PCR products were subjected to sequencing analysis.

Statistical analysis

The element concentrations presented in this study are the mean ± SD obtained from five replicate measurements of individuals using SAS software. One-way analysis of variance was performed to determine the influence of elevational microhabitats on elemental composition in *U. aprina* colonies. A $P\text{-}value < 0.01$ was considered significant. Duncan's multiple range test was used to compare the means. All of these statistical analyses were carried out using Excel 2019 and SAS 9.2 software package. For correlation analyses, we performed Pearson correlation coefficient analysis in the meta-analysis module of Metaboanalyst 5.0 and point-biserial correlation analysis using SciPy and pandas Python libraries.

Results

Metabolomics

LC–MS/MS analysis and proposed annotation/ identification

LC–MS/MS analysis revealed 27 compounds forming the metabolic profile of *U. aprina* (Table 1). The tentative identification and annotation of these compounds were carried out according to previous studies[39–46] and Lichen Substances Database (LDB)[47]. These sources allowed for comparison of the fragmentation pattern of detected compounds with their reported counterparts. CFM-ID 4.0[48] also provided us with the predicted fragmentation pattern of compounds.

Two lichenic sugar alcohols, arabitol and D-mannitol, were detected at *m/z* 151 and *m/z* 181, respectively. Four monocyclic aromatic compounds, comprising orsellinic acid, methyl 3-hydroxyorsellinate, 5-chlorodivaricatinic acid, and 2,4-dimethoxy-6-n-heptylbenzoic acid, were also detected at *m/z* 167, *m/z* 197, *m/z* 244, and *m/z* 280, respectively, along with a singular cycloaliphatic acid (portentol, *m/z* 310) and an anthraquinone identified as fallacinal (*m/z* 297). Depsidones were represented by salazinic acid (*m/z* 387) and 3-dechlorogangaleoidin (*m/z* 377), while depsides comprised barbatic acid (*m/z* 360), lecanoric acid (*m/z* 317), evernic acid (*m/z* 331), and a

No	Molecular formula	$[M\text{-}H]^-$ *m/z*	Calculated *m/z*	MS/MS ions	Tentative identification	Type[a]
1	C5H12O5	151	152.068	131, 120, 101	Arabitol	SA
2	C8H8O4	167	168.042	124, 81, 79, 41	Orsellinic acid	M
3	C6H14O6	181	182.079	180, 101, 89, 71, 59, 54, 29	D-Mannitol	SA
4	C9H16O4	187	188.104	145, 101	4,5-Dihydroxy-2-nonenoic acid	AA
5	C6H8O7	191	192.027	147, 129	2,5-Didehydro-D-gluconic acid	AA
6	C9H10O5	197	198.052	165, 149, 121	Methyl 3-hydroxy orsellinate	M
7	–	214	–	–	Unknown	–
8	C11H13ClO4	244	244.050	199, 184, 91	5-Chlorodivaricatinic acid	M
9	C14H16O4	248	248.104	190, 145	Olivetonide	IC
10	C16H24O4	280	280.167	235, 180	2,4-Dimethoxy-6-*n*-heptylbenzoic acid	M
11	C16H10O6	297	298.047	253, 169	Fallacinal	AQ
12	C20H35O2	306	307.263	254, 180	Aliphatic acid (unidentified)	AA
13	C17H26O5	310	310.178	207, 130, 88, 57	Portentol	CA
14	C16H14O7	317	318.074	167, 149, 123, 105, 81, 79	Lecanoric acid	DD
15	C19H36O4	328	328.261	283, 240, 73, 44	Angardianic acid	AC
16	C17H16O7	331	332.090	271, 252, 188, 153, 149, 124, 106	Evernic acid	DD
17	C18H16O7	343	344.089	328, 313, 259, 231	Usnic acid	DB
18	C16H12O9	347	348.048	198, 153, 149, 136, 109, 105, 65	Papulosic acid derivative	DD
19	C19H20O7	359	360.120	181, 163, 137, 120	Barbatic acid	DD
20	C21H36O5	367	368.256	323, 279	Murolic acid	FA
21	C18H15ClO7	377	378.050	331, 263, 187, 55	3-Dechlorogangaleoidin	DN
22	C18H12O10	387	388.043	343, 269, 225, 150, 120	Salazinic acid	DN
23	C24H20O10	467	468.106	168, 167, 149, 123	Gyrophoric acid	TD
24	C25H22O10	481	482.121	313, 269, 181, 167, 163, 137	Ovoic acid	TD
25	C24H20O11	483	484.101	184, 183, 168, 167, 149, 139, 97	Hiascic acid	TD
26	C25H22O11	497	498.116	348, 198, 197, 154, 153, 149	Methylhiascic acid	TD
27	C40H56O2	567	568.428	375, 197	Lutein	TP

Table 1. LC–MS/MS characterization of *U. aprina*'s metabolic profile. [a]Metabolite type → *SA* sugar alcohol, *M* monocyclic aromatic compound, *AA* aliphatic acid, *IC* isocoumarin, *AQ* anthraquinone, cycloaliphatic acid, *DD* didepside, *DB* dibenzofuran, *FA* fatty acid, *DN* depsidone, *TD* tridepside, *TP* terpenoid.

papulosic acid derivative (*m/z* 347). A dibenzofuran (usnic acid, *m/z* 343), a triterpenoid (lutein, *m/z* 567), and a fatty acid tentatively assigned as murolic acid (*m/z* 367) were detected. The identification also confirmed four tridepsides: gyrophoric acid (*m/z* 467), ovoic acid (*m/z* 481), hiascic acid (*m/z* 483), and methyl hiascic acid (*m/z* 497). Olivetonide, a lichenic isocoumarin, was identified at *m/z* 248. An uncharacterized compound (*m/z* 214) remains unresolved. All elucidated structures are presented in Fig. S1.

Multivariate analysis and pattern recognition

We performed chemometric and statistical analyses using the mass feature data. The results are provided in Fig. 2. Accordingly, in unsupervised dimensionality reduction, the PCA scores plot showed five clusters, mostly overlapping. The relative separation of these clusters was due to the differences in ion intensities since the metabolic profiles of all samples were identical. The PCA scores analysis (PC1 + PC2) explained 34.2% of the variations (Fig. 2a). The biplot, which includes the loadings, shows the most influential compounds creating the differences in PCA (Fig. S2). We also used the Pearson correlation coefficient to check if there were any correlations between different features. The correlation heatmap has been provided in Fig. S3. In Fig. S4, a heatmap has been presented based on hierarchical cluster analysis showing the similarities of samples from the same or varied elevations. In clustering analysis, Euclidean distance was used as the similarity metric, and Ward's linkage method was applied as the clustering algorithm.

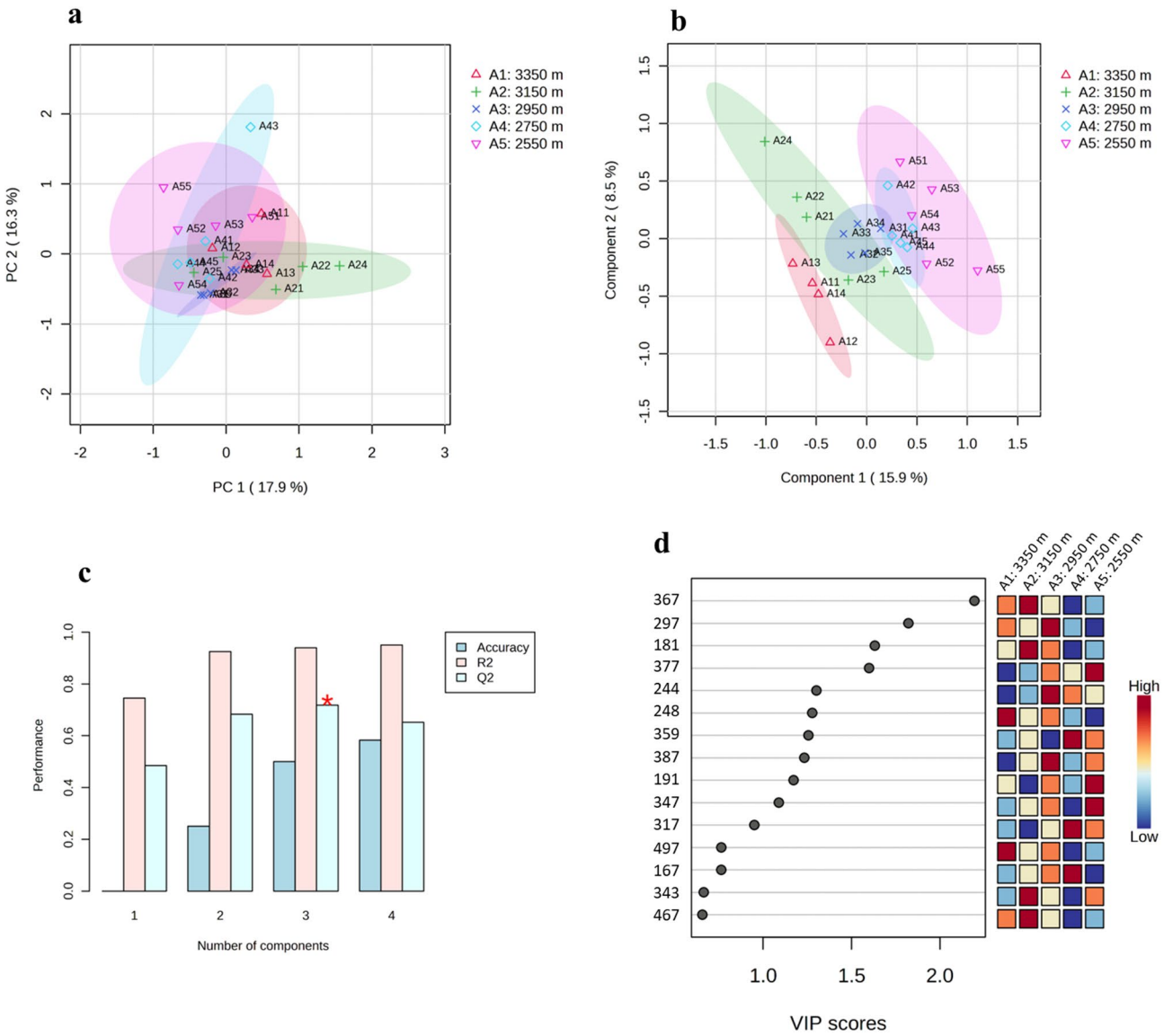

Fig. 2. Multivariate statistical analyses of metabolic profiles of different *U. aprina* colonies: (**a**) PCA scores plot; (**b**) PLS-DA scores plot; (**c**) The performance overview of different principal components in PLS-DA model; (**d**) Important metabolomic features identified by PLS-DA (The colored boxes on the right indicate the relative intensity of the corresponding metabolite in each group under study).

To obtain the specific chemical markers using supervised dimensionality reduction, PLS-DA was performed based on the mass features (Fig. 2b). The quality of the model is shown by R2 and Q2 values, 0.93 and 0.68 (Fig. 2c), showing the goodness of fit and predictability of the model, respectively. The low value of Q2 suggests that the model is of normal predictive ability and not a strong one. According to the PLS-DA scores plot (Fig. 2b), in this model, PC_1 explained 15.9% and the second PC represented 8.5% of the total variations. The first two components accounted for 24.4% of the differences. With regards to discriminating compounds, the values of Variable Importance in the Projection (VIP) show the most influential compounds (Fig. 2d). Variables with VIP scores > 1 are considered the most important ones as regards the lichen colonies' discrimination.

Elemental composition

A broad range of elements, including rare earth elements, were investigated, and a total of 33 mineral elements could simultaneously be detected and measured in our samples, including Al, As, B, Ba, Ca, Ce, Co, Cr, Cu, Fe, Ge, K, La, Li, Mg, Mn, Na, Nb, Nd, Ni, P, Pb, Pr, Rb, S, Sc, Se, Sr, Ti, V, Y, Zn, Zr (Table 2).

We subjected the dataset to unsupervised (PCA) and supervised (PLS-DA) multivariate analyses. The results are presented in Fig. 3. PCA scores plot (Fig. 3a) shows that the first two PCs account for 57.5% of the total variations (PC1 = 36% + PC2 = 21.5%). A distinct separation can be seen between the samples from different altitudes. PCA biplot (Fig. S5) (scores + loadings) shows the elements contributing effectively to the separation of the samples. To determine the most influential discriminators and make better use of our ionomics data to classify samples from different altitudes, we performed a PLS-DA modeling for 33 detected elements from 24 lichen colonies. In the PLS-DA scores plot (Fig. 3b), the first two components explained 52.9% of the total variations. As shown in Fig. 3c, R2 and Q2 were 0.97 and 0.91 respectively, showing the suitable goodness of fit and strong predictability of the model. According to VIP scores (Fig. 3d), 14 elements showed scores above 1.

Element (ppm)	A1: 3350 m (n = 4)	A2: 3150 m (n = 5)	A3: 2950 m (n = 5)	A4: 2750 m (n = 5)	A5: 2550 m (n = 5)
Al	2840.6 ± 556.74^{a}	2461.9 ± 624.27^{a}	1774.1 ± 166.77^{a}	2061 ± 733.99^{a}	2081 ± 498.18^{a}
As	3.62 ± 0.55^{b}	3.84 ± 0.79^{b}	3.09 ± 0.31^{b}	3.62 ± 0.52^{b}	5.79 ± 1.12^{a}
B	20.54 ± 2.62^{a}	17.44 ± 1.36^{b}	16.41 ± 1.33^{b}	16.55 ± 1.47^{b}	15.54 ± 0.99^{b}
Ba	13.17 ± 1.82^{a}	12.29 ± 1.72^{ab}	9.18 ± 0.69^{c}	10.13 ± 1.63^{bc}	9.64 ± 1.80^{c}
Ca	2720 ± 168.71^{a}	2541.9 ± 317.46^{a}	2545.4 ± 249.97^{a}	2101.6 ± 391.12^{b}	1534.7 ± 192.19^{c}
Ce	6.34 ± 1.24^{b}	7.27 ± 1.66^{b}	5.69 ± 0.65^{b}	7.15 ± 2.04^{b}	10.34 ± 1.68^{a}
Cu	8.61 ± 0.70^{b}	9.47 ± 2.10^{b}	9.22 ± 1.32^{b}	10.12 ± 0.76^{b}	12.21 ± 1.16^{a}
K	4038.6 ± 256.88^{a}	3467.6 ± 287.32^{a}	3785.2 ± 217.60^{a}	3630.6 ± 478.89^{a}	3577.1 ± 250.64^{a}
La	2.80 ± 0.59^{b}	3.18 ± 0.68^{b}	2.46 ± 0.26^{b}	3.17 ± 0.88^{b}	4.39 ± 0.74^{a}
Mg	1642.9 ± 212.83^{a}	1406.4 ± 252.09^{ab}	1227.2 ± 84.08^{bc}	1112.9 ± 194.22^{c}	1085.6 ± 163.45^{c}
Nd	2.71 ± 0.54^{b}	3.12 ± 0.68^{b}	2.48 ± 0.28^{b}	3.17 ± 0.85^{b}	4.39 ± 0.66^{a}
Ni	8.08 ± 1.80^{a}	8.73 ± 2.59^{a}	6.14 ± 0.84^{a}	7.01 ± 1.59^{a}	8.78 ± 1.76^{a}
P	805.47 ± 58.79^{a}	692.54 ± 34.61^{a}	775.45 ± 81.86^{a}	706.39 ± 174.68^{a}	635.26 ± 88.52^{a}
Pr	0.39 ± 0.45^{b}	0.78 ± 0.16^{ab}	0.39 ± 0.36^{b}	0.55 ± 0.52^{b}	1.11 ± 0.17^{a}
S	1835.48 ± 69.41^{b}	1675.69 ± 94.54^{b}	1846.9 ± 97.66^{a}	1582.99 ± 145.14^{b}	1626.08 ± 124.93^{b}
Se	0.69 ± 0.53^{b}	1.07 ± 0.16^{ab}	0.86 ± 0.55^{b}	1.20 ± 0.20^{ab}	1.51 ± 0.40^{a}
Sr	14.21 ± 1.18^{a}	14.07 ± 1.59^{a}	12.24 ± 0.93^{ab}	10.88 ± 2.19^{bc}	9.38 ± 0.59^{c}
Zn	52.06 ± 4.00^{a}	42.24 ± 2.34^{bc}	45.8 ± 2.50^{b}	37.48 ± 4.17^{d}	38.38 ± 3.27^{cd}
Cr	9.41 ± 2.07^{a}	8.60 ± 1.84^{a}	9.52 ± 1.14^{a}	7.48 ± 1.54^{a}	10.57 ± 0.91^{a}
Fe	3156.9 ± 625.73^{a}	2835.8 ± 692.10^{a}	2034.3 ± 191.10^{b}	2053.8 ± 352.78^{b}	2433.7 ± 567.17^{ab}
Co	1.71 ± 0.42^{ab}	1.91 ± 0.59^{ab}	1.4 ± 0.22^{b}	1.56 ± 0.20^{b}	2.28 ± 0.48^{a}
Ga	3.32 ± 0.61^{b}	3.86 ± 1.00^{b}	3.02 ± 0.45^{b}	3.97 ± 0.51^{ab}	4.87 ± 0.67^{a}
Li	3.87 ± 1.18^{ab}	3.01 ± 1.20^{bc}	2.22 ± 0.59^{c}	2.38 ± 0.60^{bc}	4.63 ± 1.46^{a}
Mn	52.02 ± 11.31^{a}	46.20 ± 9.70^{ab}	35.73 ± 4.28^{bc}	32.33 ± 5.14^{c}	36.38 ± 6.84^{bc}
Na	167.37 ± 46.63^{a}	138.49 ± 30.79^{a}	168.32 ± 19.63^{a}	129.58 ± 27.01^{a}	179.66 ± 22.23^{a}
Nb	1.28 ± 0.34^{a}	1.19 ± 0.50^{a}	0.49 ± 0.46^{b}	1.31 ± 0.57^{a}	1.62 ± 0.49^{a}
Pb	6.17 ± 0.43^{b}	6.06 ± 0.41^{b}	6.06 ± 0.31^{b}	6.62 ± 0.75^{b}	9.47 ± 0.45^{a}
Rb	2.97 ± 1.07^{a}	2.95 ± 1.14^{a}	2.48 ± 1.59^{a}	3.02 ± 1.97^{a}	3.38 ± 1.48^{a}
Sc	1.16 ± 0.20^{ab}	1.26 ± 0.42^{ab}	0.89 ± 0.08^{b}	1.17 ± 0.26^{ab}	1.59 ± 0.35^{a}
Ti	95.12 ± 25.10^{a}	87.21 ± 28.05^{a}	58.15 ± 6.33^{a}	76.49 ± 22.77^{a}	86.18 ± 26.30^{a}
V	7.99 ± 1.45^{a}	7.08 ± 1.29^{ab}	4.84 ± 0.36^{c}	4.72 ± 0.58^{c}	5.61 ± 1.41^{bc}
Y	1.39 ± 0.08^{a}	1.30 ± 0.11^{a}	1.28 ± 0.08^{a}	1.33 ± 0.10^{a}	1.34 ± 0.08^{a}
Zr	1.84 ± 0.47^{a}	1.59 ± 0.18^{ab}	1.37 ± 0.22^{b}	1.63 ± 0.19^{ab}	1.87 ± 0.15^{a}

Table 2. Elemental composition of *U. aprina* samples from five different altitudes analyzed by ICP-MS. Values are mean ± SD; Various letters in each row denote significant statistical differences between samples.

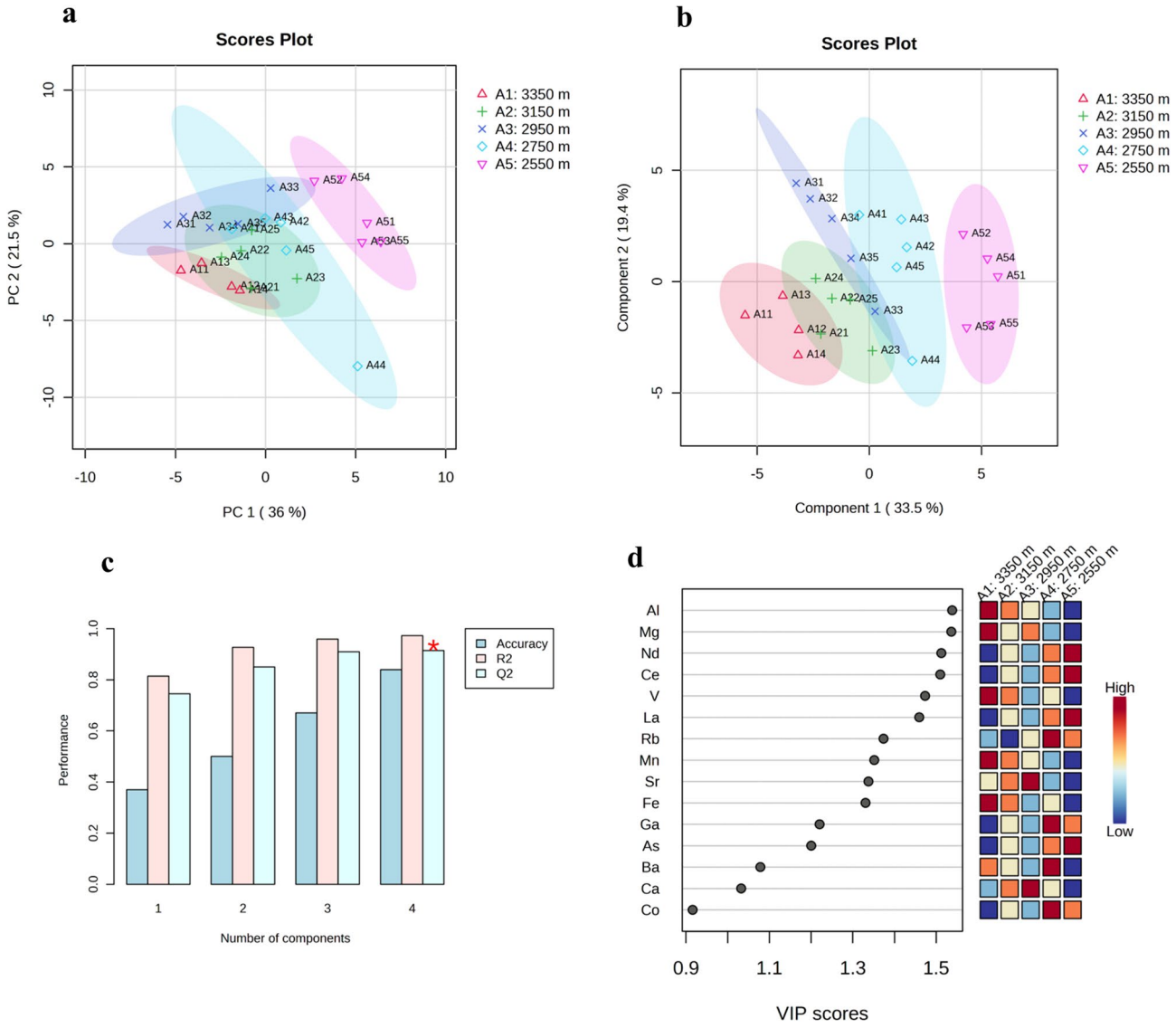

Fig. 3. Multivariate statistical analyses of the elemental composition of different *U. aprina* colonies: (**a**) PCA scores plot, (**b**) PLS-DA scores plot, (**c**) The performance overview of different principal components in PLS-DA model, (**d**) Important elemental markers identified by PLS-DA (The colored boxes on the right indicate the relative concentration of the corresponding element in each group under study).

We considered these 14 elements, namely Ca, Ba, As, Ga, Fe, Sr, Mn, Rb, La, V, Ce, Nd, Mg, and Al (in increasing order of VIP scores), the most influential discriminators between lichen colonies from different altitudes. The correlation analysis of elements (based on the Pearson correlation coefficient) has been represented in Fig. S6. In Fig. S7, we have provided the result of clustering analysis showing the similarities of different colonies in terms of their elemental compositions.

U. aprina's microbial profile

Lists of the identified endolichenic fungi, lichen-associated bacteria, and their accession numbers are given in our online supplementary material (Tables S1 and S2). The heatplot (Fig. 4) shows the microbial variations among the colonies from different elevations. There is no regular pattern in the results but interestingly the samples from the highest elevation (A1: 3350 m) possessed very few endolichenic fungi compared with those from the lowest elevation (A5: 2550 m). It should be noted that the endolichenic fungi isolated from A1 and A2 colonies displayed weak sporulation, which limited their identification. This was in contrast to the good sporulation of endolichenic fungi isolated from the A3, A4, and A5 colonies, leading to their convenient identification. According to the heatplot (Fig. 4), some of the endolichenic fungi were similar between different altitudes. For instance, *Alternaria multiformis* was isolated from samples of A2, A3, A4, and A5 colonies. However, *Fusarium incarnatum*. was detected in samples from A3 and A4 colonies, and *Curvularia neegaardii* was only isolated from A2 colonies. Similarly, another strain of *Fusarium* sp. was only observed in A3 colonies. All in all, endolichenic fungi were present at different heights without any regular pattern. Eight morphologically distinct bacteria were

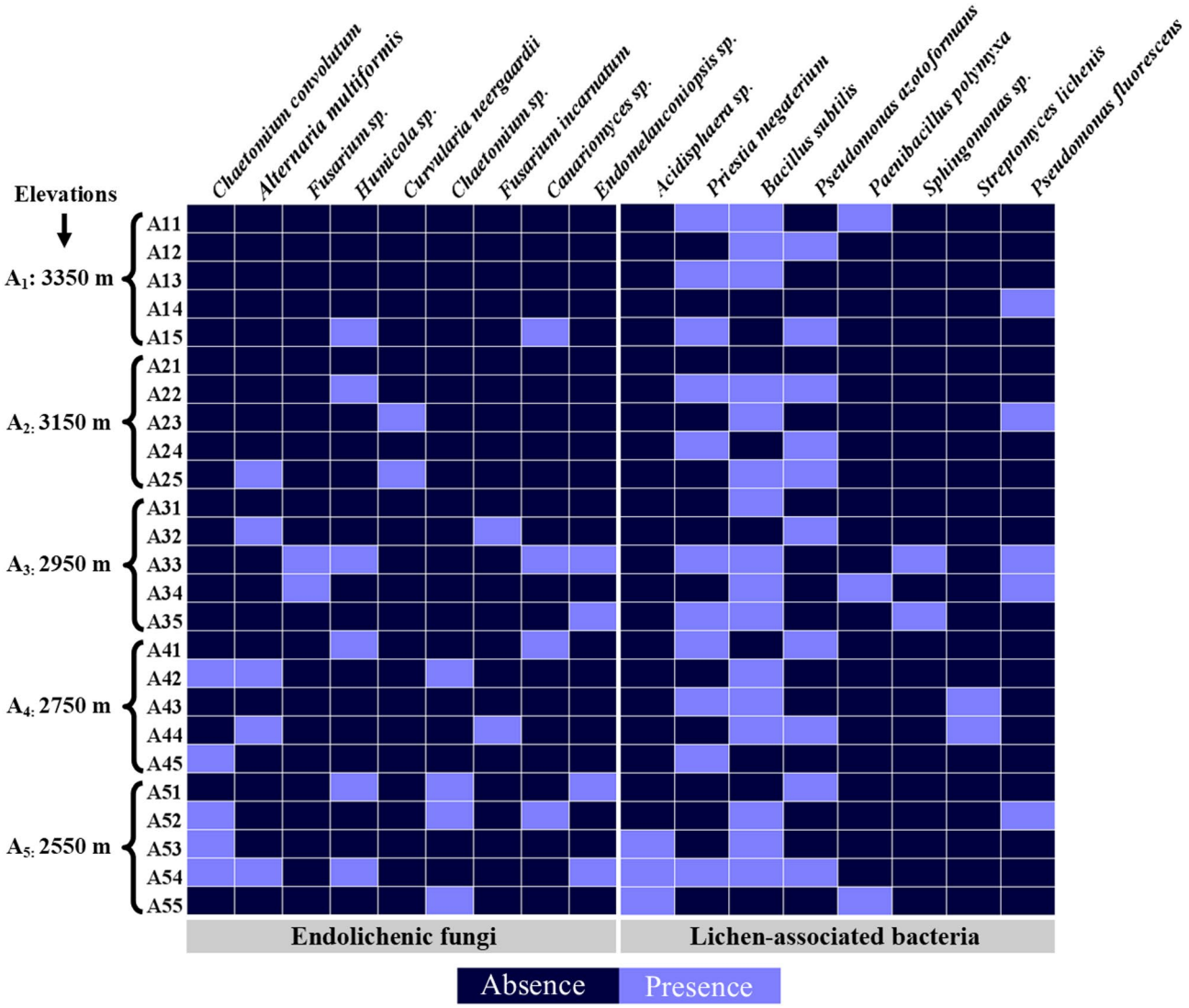

Fig. 4. Significant variations in the microbial composition of *U. aprina* colonies across various elevations.

also isolated from the lichen samples. In addition to phenotypic and biochemical tests, we also used 16S rRNA gene sequencing. Polymerase chain reaction with a general primer formed a single band of about 1500 bp in selected strains on agarose gel. The BLAST search of GenBank for all isolates provided a similarity above 99% between the bacteria tested and those detected in Genbank. The results of biochemical tests of the selected species are shown in Tables S3–S10. As shown in the heatplot (Fig. 4), *Priestia megaterium*, *Bacillus subtilis*, and *Pseudomonas azotoformans* were dominant bacteria at all heights. *Streptomyces lichenis* was only detected in A4 colonies. *Sphingomonas* sp. was only observed in A3 colonies. Similarly, *Acidisphaera* sp. was only observed in A5 colonies.

Discussion

Lichen-environment interactions are complex and dynamic. It is common knowledge that environmental conditions change in line with topographic shifts. For instance, when the elevation of a particular location changes, many environmental factors may change as well, including temperature, moisture, UV intensity, and the amount and type of precipitation. Lichens perceive these environmental variations and respond commensurately. And a lichen's response may comprise physiological, biochemical, biological, morphological, and metabolic variations. All these variations are the staple components of what we call environmental fitness mechanism, and none of them acts individually. So, many endolichenic shifts may occur as a result of changes in a lichen's surroundings. In this study, we looked at lichen-environment interactions from a slightly different angle and investigated three important endolichenic traits: (a) elemental composition, (b) microbiome, and (c) metabolome. Our findings showed that these endolichenic traits change along the selected altitudinal gradient.

In respect of elemental composition, multivariate data analysis showed clear distinctions among colonies from different elevations. Surprisingly, the PCA scores plot showed a marked difference between the colonies of the highest and lowest elevations (Fig. 3a), and the PLS-DA scores plot showed a left-to-right separation trend,

from the highest elevation (A1) to the lowest (A5) (Fig. 3b). As shown in the heatmap clustering (Fig. S7), the colonies from the lowest elevation (A5) had lower concentrations of Ba, Mn, V, Al, Fe, Mg, Ca, Sr, K, P, S, B, and Zn, whereas colonies from the other elevations, especially the highest (A1), showed higher concentrations of these elements. A5 colonies had the highest concentrations of As, Ce, Cu, La, Nd, Pr, Se, Co, Ga, Li, Pb, and Sc, while A1 colonies possessed the highest concentrations of B, Ba, Ca, K, Mg, P, Sr, Zn, Fe, Mn, Ti, V, and Y (Table 2). Interestingly, most of the high-concentration elements from A1 colonies are Lithophiles, the fundamental sources of rock-forming minerals[49]. But heavy metals make up the majority of the high-concentration elements, such as As, Cu, La, Co, Ga, and Pb, in A5 colonies. This may be due to the fact that the highest elevation in this study is almost devoid of anthropogenic alterations and activities, whereas the lowest elevation is much closer to potential sources of contamination such as vehicular traffic, which may account for the higher concentration of Pb in A5 colonies. Our findings showed that *U. aprina* colonies accumulate different concentrations of various elements. We know that lichens absorb and accumulate elements in different ways. They can take up cations from their substrate over the entire lower cortex or trap soil or atmospheric particles in their interwoven medulla[50]. They are also likely to absorb/adsorb elements from precipitation, dew, and fog[51]. The morphology and chemistry of a thallus may also be important contributing factors affecting the accumulation of different elements. For example, Upreti and Pandev[52] compared the accumulation capacity of *U. aprina* and *Umbilicaria decussata*. The latter showed significantly higher levels of heavy metals, including Fe, Cu, Pb, and Cr. The authors concluded that *U. decussata*'s morphology better suits the accumulation of heavy metals since it has a thin thallus providing a large surface area to dry weight ratio in comparison with *U. aprina*. This may highlight the possible role of thallus morphology in the elemental variations in our work. *U. aprina*'s thallus shows a high morphological plasticity even in a limited alpine area. All in all, several factors may affect the amount and type of elements in different *U. aprina* colonies, such as exposure to environmental pollutants, morphology, and lichen chemistry. It is clear that investigating other influencing factors, including ultraviolet radiation, temperature, precipitation, and others, requires more detailed and comprehensive studies.

As mentioned, in another part of this study, we focused on the microbial variations of *U. aprina* colonies from different altitudes. Some possible contributing factors driving lichen microbial variations have been reported to date. Host-specific factors, such as thallus morphology, structure, texture, and substrate, may influence the microbial communities of different lichen species[53]. The geographical difference has also been considered effective on microbial diversity. For example, Zhang et al.[54] reported phylogenetic dissimilarities between Arctic and non-Arctic microbial communities. Elevation has also proven a significant environmental factor influencing the microbial communities of lichens[55,56]. In an interesting study, Wang et al.[57] investigated the possible effect of site and altitude on the microbial community of *Hypogymnia hypotrypa* using a culture-independent method, IlluminaMiSeq sequencing. Their findings showed meaningful microbial variations with changes in altitude and sampling site. Generally, elevation seems to impact the richness and diversity of microbial communities in lichens. Higher elevations are likely to reduce the richness and diversity of microbial communities in lichens[58]. This may stem from the increase in the adversity of environmental conditions at higher altitudes. Previous studies have pointed out the possible roles of microbial communities in lichens' biological and physiological processes of lichens, including metabolism, water relations, thallus architecture, degradation processes[59,60], and defensive mechanisms[61]. These microbial communities comprise two groups: (i) a species-specific group (or core group) and (ii) a site-specific group. The latter may change under different climatic and geographical conditions[19–21,23], which corresponds with its possible role in the environmental fitness of lichens. In other words, such changes may prepare lichens for environmental adaptations[62,63]. So, when a lichen is subjected to environmental stresses and climate change, the whole micro-ecosystem will undergo some alterations.

Given that environmental and endolichenic factors (i.e., elemental composition and microbial profile) were different among *U. aprina* colonies from various elevations, we expected metabolic variations as well. There is a widespread belief that lichens owe part of their environmental resilience to their secondary metabolism[64,65]. In other words, they produce a vast spectrum of bioactive compounds as part of their environmental fitness mechanism. Accordingly, if the lichen metabolome has an adaptive role, then we should see metabolic changes under different environmental and endolichenic conditions. Different colonies of *U. aprina* from various elevations showed variations in their metabolic status (Fig. 2). As shown in Fig. 2b, there is a clear distinction between the colonies from the highest elevation (A1) and those from the lowest elevation (A5). This suggests that an increase in geographical differences may result in higher variations in the metabolic status of *U. aprina*. It should also be noted that fluctuations in the concentration of different metabolites do not follow a regular pattern along an altitudinal gradient, especially a linear pattern. This was confirmed in our work with an investigation into the potential correlations between the relative concentrations of secondary metabolites and elevation. Although there were metabolic variations among colonies from different elevations based on untargeted metabolomics (Fig. 2), we could not find a meaningful ($P < 0.05$) strong correlation (i.e., $r > 0.6$) between the relative concentrations of different secondary metabolites and elevations (Table S11). However, several metabolites showed a meaningful ($P < 0.05$) moderate (i.e., $0.4 < r < 0.6$) correlation with elevation. D-Mannitol (*m/z* 181), murolic acid (*m/z* 367), fallacinal (*m/z* 297), and olivetonide (*m/z* 248) showed moderate positive correlations, while 5-chlorodivaricatinic acid (*m/z* 244), barbatic acid (*m/z* 359), and lecanoric acid (*m/z* 317) showed moderate negative correlations. Interestingly, gyrophoric acid, the main *Umbilicaria* tridepside, has shown a meaningful and negative correlation with altitude[66]. In our study, gyrophoric acid did not show any meaningful correlation with elevation, but lecanoric acid, a precursor in the synthesis of gyrophoric acid, was negatively correlated with elevation. It seems that metabolite concentration does not always follow a regular linear pattern in response to elevation rise or fall and that each compound may respond to such environmental factors in a more or less independent manner. Such a compound-specific response of the lichen metabolome to elevational gradients has been studied elsewhere[67]. Our findings also confirm such responses in *U. aprina*'s metabolome.

Pearson correlation analysis was also performed for the metabolites and elements. The results have been provided in our online supplementary file (Fig. S8). Although a few of the elements, such as Fe, Na, and Pb, did not show any meaningful correlations ($P < 0.05$) at all, other elements showed significant correlations. Noticeably, orsellinic acid was negatively correlated with several elements including As, Ce, Co, Cr, La, Li, Nd, Ni, Pr, and Y. Murolic acid was positively correlated with the concentration of many elements, including Ba, Ce, Co, Cu, Ga, La, Li, Nb, Nd, Ni, Pr, Rb, Sc, and Ti. S was the only element negatively correlated with murolic acid. Similarly, lecanoric acid showed a negative correlation with Ca, V, Mg, Mn, Sr, Y, Al, and B. D-mannitol showed a positive correlation with Zn, Sr, S, Ca, and Mg, and was also negatively correlated with Rb, Ga, and Nb. We could also see a positive correlation between fallacinal and K, Mg, S, Sr, and Zn. Olivetonide and methylhiascic acid were similarly correlated positively with P, S, and Y. A prominent example of correlation in our results can be seen in the case of yttrium (Y). Yttrium's concentration showed the highest positive correlation (0.71) with methylhiascic acid (*m/z* 497) compared to other correlation pairs. As mentioned earlier, it was also positively correlated with olivetonide (*m/z* 248) and gyrophoric acid (*m/z* 467) with coefficients greater than 0.6 and about 0.6, respectively. Interestingly, it showed a negative correlation (> -0.6) with lecanoric acid (*m/z* 317). There is no evidence of the possible effects of yttrium on lichen physiology and biology. Yttrium is a rare earth element (REE) with possible negative effects on the growth and physiological characteristics of algae[68] and positive effects on photosynthesis and water relations in plants[69].

We may not reach any meaningful conclusions based on simple correlation analyses but several studies have emphasized the possible role of different elements in the chemical alterations of lichens. Białońska and Dayan[70], for example, investigated the effects of industrial pollution on the chemical composition of *Hypogymnia physodes*. They conducted a transplantation experiment, moving lichen samples from a clean reference site to an industrialized region. The study found significant changes in the chemistry of the transplanted lichens compared to the reference samples. Lichen transplants exposed to high chromium levels showed reductions in physodic acid, hydroxyphysodic acid, and atranorin concentrations. Likewise, lichens transplanted to another heavily polluted site near a zinc-lead smelter displayed a decrease in physodic acid concentration due to the accumulation of cadmium, lead, and zinc. There is also evidence of the possible correlation of usnic acid concentration in *Cladonia mitis* with heavy metal content[71]. Other studies have also confirmed the possible effect of chemical variations on the bioaccumulation capacity of lichens. For instance, Malaspina et al.[72] researched the bioaccumulation capacity of two chemical varieties of the lichen *Pseudevernia furfuracea*. In their study, both chemical varieties of *Pseudevernia furfuracea* showed a high bioaccumulation capacity for heavy metals, including copper, zinc, lead, and cadmium. However, there were variations in the accumulation patterns between the two chemical varieties. The authors concluded that the chemical differences between the two varieties may play a role in their bioaccumulation capacities. On the whole, lichens may increase the biosynthesis of their secondary metabolites as a stress-repressive strategy. For instance, *Diploschistes muscorum* might increase the production of orsellinic acid, diploschistesic acid, and lecanoric acid under Pb accumulation. These metabolites, possessing antioxidant properties that counteract the oxidative damage caused by heavy metals, might contribute to the overall stress response of this lichen[73]. There is, however, evidence of zero chemical alterations of lichens under heavy metal pollution. Despite being a notable stress-resilient lichen species, *Cladonia rei* did not show any chemical shifts under heavy metal accumulation[74].

The chemical fluctuations of *U. aprina* colonies in our study may not merely be induced by elemental differences. An interplay of different endolichenic and environmental factors may control the chemical diversity of lichens[75]. We further used point-biserial correlation analysis to see the possible associations between the metabolites and microbiome. The results can be observed in our online supplementary material (Tables S12–S38). Some moderate and meaningful correlations were found between the occurrence (i.e., presence or absence) of some microbes and the relative intensity of different metabolites. Notably, *Alternaria multiformis* showed moderate positive correlations with 5-chlorodivaricatinic acid, olivetonide, barbatic acid, 3-dechlorogangaleoidin, hiascic acid, and methylhiascic acid. In addition, a moderate positive correlation was observed between *Sphingomonas* sp. and both D-mannitol and fallacinal.

Acidisphaera sp. showed positive correlations with 2,5-didehydro-D-gluconic acid and lutein. *Fusarium* sp. was positively correlated with 2,4-dimethoxy-6-*n*-heptylbenzoic acid and fallacinal. *Chaetomium convolutum* showed positive correlations with barbatic acid and hiascic acid. *Paenibacillus polymyxa* was positively correlated with *m/z* 214 and negatively correlated with gyrophoric acid. There were also positive correlations between *Streptomyces lichenis* and orsellinic acid, *Pseudomonas azotoformans* and evernic acid. *Humicola* sp. and *Priestia megaterium* were negatively correlated with D-mannitol and papulosic acid derivative, respectively.

Considering that the lichen microbiome has been reported to be responsible for various physiological and biological lichenic processes, the metabolite-microbiome correlation remains to be further investigated. Research has shown the upregulation of various stress-adapting genes in microbial communities of lichens under different environmental stresses[76,77]. So, the microbiome may play an indirect role in the biosynthesis of lichenic substances. Some studies have even reported the capability of some endolichenic and lichenicolous fungi of producing common lichenic substances. Gyrophoric acid, for instance, was detected in *Sclerococcum sphaerale* and *Skyttea nitschkei*, two lichencolous fungi[78]. It was also reported from cultures of a *Humicola* sp. isolated from soil samples[79]. We have also identified a *Humicola* sp. in our *U. aprina* colonies (Fig. 4). Since *U. aprina* is a mass producer of gyrophoric acid, as a future direction, it is worth researching whether its *Humicola* fungal strain produces gyrophoric acid or not. However, it should be noted that we could not recognize any meaningful correlation between the relative concentration of gyrophoric acid and the presence or absence of *Humicola* sp. (Table S34).

The study looked into the complex and dynamic nature of lichen-environment interactions. We focused on three endolichenic traits, including elemental composition, microbiome, and metabolome, and examined their variations along an altitudinal gradient. These traits showed significant changes among *U. aprina* colonies

from different elevations. Investigating the possible interplay of different endolichenic traits may be a better way for elucidating the complex lichen-environment interactions. For instance, inorganic elements may impact the enzymatic activities involved in the metabolic pathways of lichens. Such an interplay could result in some clarifications about the correlations we observed between the relative intensity of some secondary metabolites and inorganic elements. But it is worth mentioning that the interplays of endolichenic traits under different environmental conditions in such a long-lived symbiotic organism might be balanced by a variety of factors. This can explain why we could not detect any strong correlations between the studied endolichenic traits. On the whole, lichens are extremophile creatures, which means they can thrive in extreme environments unfit for other creatures' habitation, such as plants. This is to say lichens are good at adapting to harsh environments. Their unique and high level of adaptation may stem from their genome plasticity[24]. The existence of some climate-associated biosynthetic gene clusters has been confirmed in some populations of *Umbilicaria pustulata*[80]. This interesting discovery shows that lichens are able to produce environment-specific metabolites. Various populations of *Umbilicaria phaea* and *U. pustulata* have even shown variations in their gene content under different environmental conditions across altitudinal gradients[81]. But there remains a question to be answered: does a particular species of lichen, such as *U. aprina*, have different active biosynthetic gene clusters along an altitudinal gradient in a limited alpine area? Another interesting future step would be integrating untargeted metabolomics and genomic studies to unravel the underlying mechanisms of chemical alterations of lichens under microclimatic differences. Understanding these associations can provide valuable insights into lichens' adaptive mechanisms and their responses to environmental stresses. Future studies can delve deeper into the indirect role of the microbiome in the biosynthesis of lichenic substances and explore the intricate genetic and biochemical interactions within lichen communities under different environmental conditions. Overall, this study contributes to the growing body of knowledge on lichen-environment interactions and provides a foundation for further exploration of the fascinating world of lichens and their intricate environmental adaptations.

Data availability

The datasets used and/or analyzed during the current study are available from the corresponding author upon reasonable request.

Received: 5 January 2025; Accepted: 19 May 2025
Published online: 28 May 2025

References

1. Lücking, R., Leavitt, S. D. & Hawksworth, D. L. Species in lichen-forming fungi: Balancing between conceptual and practical considerations, and between phenotype and phylogenomics. *Fungal Divers.* **109**, 99–154 (2021).
2. Gheza, G. et al. Morphological and chemical traits of *Cladonia* respond to multiple environmental factors in acidic dry grasslands. *Microorganisms* **9**, 1–12 (2021).
3. Zraik, M., Booth, T. & Piercey-Normore, M. D. Relationship between lichen species composition, secondary metabolites and soil pH, organic matter, and grain characteristics in Manitoba. *Botany* **96**, 267–279 (2018).
4. Culberson, W. L. Analysis of chemical and morphological variation in the *Ramalina siliquosa* species complex. *Brittonia* **19**, 333–352 (1967).
5. Culberson, W. L., Culberson, C. F. & Johnson, A. Speciation in lichens of the *Ramalina siliquosa* complex (Ascomycotina, Ramalinaceae): Gene flow and reproductive isolation. *Am. J. Bot.* **80**, 1472–1481 (1993).
6. Culberson, W. L. & Culberson, C. F. Habitat selection by chemically differentiated races of lichens. *Science* **1979**(158), 1195–1197 (1967).
7. Swanson, A., Fahselt, D. & Smith, D. Phenolic levels in *Umbilicaria americana* in relation to enzyme polymorphism, altitude and sampling date. *Lichenologist* **28**, 331–339 (1996).
8. Hamada, N. The content of lichen substances in *Ramalina siliquosa* cultured at various temperatures in growth cabinets. *Lichenologist* **16**, 96–98 (1984).
9. Hamada, N. The effect of temperature on the content of the medullary depsidone salazinic acid in *Ramalina siliquosa* (lichens). *Can. J. Bot* **60**, 383–385 (1982).
10. Hamada, N. Environmental factors affecting the content of usnic acid in the lichen mycobiont of *Ramalina siliquosa*. *Bryologist* **94**, 57 (1991).
11. Armaleo, D., Zhang, Y. & Cheung, S. Light might regulate divergently depside and depsidone accumulation in the lichen *Parmotrema hypotropum* by affecting thallus temperature and water potential. *Mycologia* **100**, 565–576 (2008).
12. BeGora, M. D. & Fahselt, D. Usnic acid and atranorin concentrations in lichens in relation to bands of UV irradiance. *Bryologist* **104**, 134–140 (2001).
13. Bjerke, J. W., Lerfall, K. & Elvebakk, A. Effects of ultraviolet radiation and PAR on the content of usnic and divaricatic acids in two arctic-alpine lichens. *Photochem. Photobiol. Sci.* **1**, 678–685 (2002).
14. Bjerke, J. W., Zielke, M. & Solheim, B. Long-term impacts of simulated climatic change on secondary metabolism, thallus structure and nitrogen fixation activity in two cyanolichens from the Arctic. *New Phytol.* **159**, 361–367 (2003).
15. Bjerke, W. & Dahl, T. Distribution patterns of usnic acid-producing lichens along local radiation gradients in West Greenland. *Nova Hedwigia* **75**, 487–506 (2002).
16. Norouzi, H., Azizi, A., Gholami, M., Sohrabi, M. & Boustie, J. Chemotype variations among lichen ecotypes of *Umbilicaria aprina* as revealed by LC-ESI-MS/MS: a survey of antioxidant phenolics. *Environ. Sci. Pollut. Res.* **27**, 40296–40308 (2020).
17. Bjerke, J. W., Elvebakk, A., Domínguez, E. & Dahlback, A. Seasonal trends in usnic acid concentrations of Arctic, alpine and Patagonian populations of the lichen *Flavocetraria nivalis*. *Phytochemistry* **66**, 337–344 (2005).
18. Neupane, B. et al. Elevational trends in usnic acid concentration of lichen *Parmelia flexilis* in relation to temperature and precipitation. *Climate* **5**, 40 (2017).
19. U'Ren, J. M., Lutzoni, F., Miadlikowska, J., Laetsch, A. D. & Arnold, A. E. Host and geographic structure of endophytic and endolichenic fungi at a continental scale. *Am. J. Bot.* **99**, 898–914 (2012).
20. Leiva, D. et al. The bacterial community of the foliose macro-lichen *Peltigera frigida* is more than a mere extension of the microbiota of the subjacent substrate. *Microb. Ecol.* **81**, 965–976 (2021).
21. Cardinale, M., Steinová, J., Rabensteiner, J., Berg, G. & Grube, M. Age, sun and substrate: Triggers of bacterial communities in lichens. *Environ. Microbiol. Rep.* **4**, 23–28 (2012).

22. Klarenberg, I. J., Keuschnig, C., Warshan, D., Jónsdóttir, I. S. & Vilhelmsson, O. The total and active bacterial community of the chlorolichen *Cetraria islandica* and its response to long-term warming in Sub-Arctic tundra. *Front. Microbiol.* **11**, 1–13 (2020).
23. Noh, H. J. et al. Microbiome in *Cladonia squamosa* is vertically stratified according to microclimatic conditions. *Front. Microbiol.* **11**, 1–13 (2020).
24. Dal Grande, F. et al. Transposable elements in the genome of the Lichen-forming fungus *Umbilicaria pustulata* and their distribution in different climate zones along elevation. *Biology (Basel)* **11**, 11010024 (2022).
25. Spribille, T. et al. Basidiomycete yeasts in the cortex of ascomycete macrolichens. *Science* **1979**(353), 488–492 (2016).
26. Grimm, M. et al. The lichens' microbiota, still a mystery?. *Front. Microbiol.* **12**, 623839 (2021).
27. Kayes, L. Chemical variation of Usnea longissima Ach. in the central Oregon coast range. *N. Am. Fungi* **3**, 1–10 (2008).
28. Ivanova, N. V., Depriest, P. T., Bobrova, V. K. & Troitsky, A. V. Phylogenetic analysis of the lichen family Umbilicariaceae based on nuclear ITS1 and ITS2 rDNA sequences. *Lichenologist* **31**, 477 (1999).
29. Davydov, E. A. et al. Umbilicariaceae (lichenized Ascomycota): Trait evolution and a new generic concept. *Taxon* **66**, 1282–1303 (2017).
30. Ryvarden, L. *Umbilicaria aprina* Nyl., a Rare Lichen. *Bryologist* **71**, 366–368 (1968).
31. Seaward, M. R. D., Sipman, H. J. M. & Sohrabi, M. A revised checklist of lichenized, lichenicolous and allied fungi for Iran. *Sauteria* **15**, 459–520 (2008).
32. Krzewicka, B., García, M. A., Johansen, S. D., Sancho, L. G. & Martín, M. P. Morphological and nuclear ribosomal DNA data support distinguishing two new species of *Umbilicaria* (Umbilicariaceae, Ascomycota) from Europe. *Lichenologist* **41**, 631–648 (2009).
33. Boonpeng, C., Sangiamdee, D., Noikrad, S. & Boonpragob, K. Influence of washing thalli on element concentrations of the epiphytic and epilithic lichen *Parmotrema tinctorum* in the tropic. *Environ. Sci. Pollut. Res.* **28**, 9723–9730 (2021).
34. Schulz, B., Wanke, U., Draeger, S. & Aust, H. J. Endophytes from herbaceous plants and shrubs: effectiveness of surface sterilization methods. *Mycol. Res.* **97**, 1447–1450 (1993).
35. Möller, E. M., Bahnweg, G., Sandermann, H. & Geiger, H. H. A simple and efficient protocol for isolation of high molecular weight DNA from filamentous fungi, fruit bodies, and infected plant tissues. *Nucleic Acids Res.* **20**, 6115–6116 (1992).
36. Biosca, E. G., Flores, R., Santander, R. D., Díez-Gil, J. L. & Barreno, E. Innovative approaches using lichen enriched media to improve isolation and culturability of lichen associated bacteria. *PLoS ONE* **11**, 1–22 (2016).
37. Schaad, N. W., Jones, J. B. & Chun, W. *Laboratory Guide for the Identification of Plant Pathogenic Bacteria* (American Phytopathological Society (APS Press), 2001).
38. Yeates, C., Gillings, M. R., Davison, A. D., Altavilla, N. & Veal, D. A. PCR amplification of crude microbial DNA extracted from soil. *Lett. Appl. Microbiol.* **25**, 303–307 (1997).
39. Calla-Quispe, E., Robles, J., Areche, C. & Sepulveda, B. Are ionic liquids better extracting agents than toxic volatile organic solvents? A combination of ionic liquids, microwave and LC/MS/MS, applied to the lichen *Stereocaulon glareosum*. *Front. Chem.* **8**, 1–7 (2020).
40. Kumar, K. et al. UPLC–MS/MS quantitative analysis and structural fragmentation study of five *Parmotrema* lichens from the Eastern Ghats. *J. Pharm. Biomed. Anal.* **156**, 45–57 (2018).
41. Posner, B., Feige, G. B. & Huneck, S. Studies on the chemistry of the lichen genus *Umbilicaria* Hoffm. *Z. Naturforsch. C* **47**, 1–9 (1992).
42. Seriña, E., Arroyo, R., Manrique, E. & Sancho, L. G. Lichen substances and their intraspecific variability within eleven *Umbilicaria* species in Spain. *Bryologist* **99**, 335–342 (1996).
43. Zlatanovića, I. et al. Chemical composition of *Umbilicaria crustulosa* and *U. cylindrica*. *Nat. Prod. Commun.* **12**, 1–2 (2017).
44. Narui, T., Culberson, C. F., Culberson, W. L., Johnson, A. & Shibata, S. A contribution to the chemistry of the lichen family umbilicariaceae (Ascomycotina). *Bryologist* **99**, 199–211 (1996).
45. Narui, T. et al. NMR assignments of depsides and tridepsides of the lichen family Umbilicariaceae. *Phytochemistry* **48**, 815–822 (1998).
46. Huneck, S. & Yoshimura, I. *Identification of Lichen Substances* (Springer, 1996). https://doi.org/10.1007/978-3-642-85243-5_2.
47. Olivier-Jimenez, D. et al. A database of high-resolution MS/MS spectra for lichen metabolites. *Sci. Data* **6**, 294 (2019).
48. Wang, F. et al. CFM-ID 40: More accurate ESI-MS/MS spectral prediction and compound identification. *Anal. Chem.* **93**, 11692–11700 (2021).
49. Haldar, S. K. Introduction. in *Platinum-Nickel-Chromium Deposits: Geology, Exploration, and Reserve Base* 1–35 (Elsevier, Amsterdam, 2017). https://doi.org/10.1016/C2014-0-00851-9.
50. Bargagli, R., Sanchez-Hernandez, J. C. & Monaci, F. Baseline concentrations of elements in the Antarctic macrolichen *Umbilicaria decussata*. *Chemosphere* **38**, 475–487 (1999).
51. Bargagli, R., Borghini, F. & Celesti, C. Elemental composition of the lichen *Umbilicaria decussata*. *Eur. Zool. J.* **67**, 157–162 (2000).
52. Upreti, D. K. & Pandev, V. Heavy metals of Antarctic lichens 1. *Umbilicaria. Feddes Repert.* **105**, 197–199 (1994).
53. Zhang, T., Wei, X. L., Zhang, Y. Q., Liu, H. Y. & Yu, L. Y. Diversity and distribution of lichen-associated fungi in the Ny-Ålesund Region (Svalbard, High Arctic) as revealed by 454 pyrosequencing. *Sci. Rep.* **5**, 1–10 (2015).
54. Zhang, T., Wei, X. L., Wei, Y. Z., Liu, H. Y. & Yu, L. Y. Diversity and distribution of cultured endolichenic fungi in the Ny-Ålesund Region, Svalbard (High Arctic). *Extremophiles* **20**, 461–470 (2016).
55. Rolshausen, G., Dal Grande, F., Otte, J. & Schmitt, I. Lichen holobionts show compositional structure along elevation. *Mol. Ecol.* https://doi.org/10.1111/mec.16471 (2022).
56. Coleine, C. et al. Altitude and fungal diversity influence the structure of Antarctic cryptoendolithic bacteria communities. *Environ. Microbiol. Rep.* **11**, 718–726 (2019).
57. Wang, Y., Zheng, Y., Wang, X., Wei, X. & Wei, J. Lichen-associated fungal community in *Hypogymnia hypotrypa* (Parmeliaceae, Ascomycota) affected by geographic distribution and altitude. *Front. Microbiol.* **7**, 1–11 (2016).
58. Wang, Q., Li, J., Yang, J., Zou, Y. & Zhao, X. Q. Diversity of endophytic bacterial and fungal microbiota associated with the medicinal lichen *Usnea longissima* at high altitudes. *Front. Microbiol.* **13**, 1–14 (2022).
59. Sargsyan, R. R., Tsurykau, A. & Panosyan, H. Lichen microbiome: Diversity biological role and biotechnological application. in *Microbes in Microbial Communities: Ecological and Applied Perspectives* 195–213 (Springer, 2022). https://doi.org/10.1007/978-981-16-5617-0_9.
60. Cernava, T. et al. Deciphering functional diversification within the lichen microbiota by meta-omics. *Microbiome* **5**, 82 (2017).
61. Cernava, T., Müller, H., Aschenbrenner, I. A., Grube, M. & Berg, G. Analyzing the antagonistic potential of the lichen microbiome against pathogens by bridging metagenomic with culture studies. *Front. Microbiol.* **6**, 1–11 (2015).
62. Eymann, C. et al. Symbiotic interplay of fungi, algae, and bacteria within the lung lichen *Lobaria pulmonaria* L. Hoffm. as assessed by state-of-the-art metaproteomics. *J. Proteome Res.* **16**, 2160–2173 (2017).
63. Grube, M. et al. Exploring functional contexts of symbiotic sustain within lichen-associated bacteria by comparative omics. *ISME J.* **9**, 412–424 (2015).
64. Gill, H., Sorensen, J. L. & Collemare, J. Lichen fungal secondary metabolites: Progress in the genomic era toward ecological roles in the interaction. In *Plant Relationships* Vol. 5398 (eds Scott, B. & Mesarich, C.) (Springer, 2023).
65. Beckett, R. P., Minibayeva, F., Solhaug, K. A. & Roach, T. Photoprotection in lichens: Adaptations of photobionts to high light. *Lichenologist* **53**, 21–33 (2021).

66. Bokhorst, S., Asplund, J. & Convey, P. Intra-specific variation in lichen secondary compounds across environmental gradients on Signy Island, maritime Antarctic. *Polar. Biol.* https://doi.org/10.1007/s00300-021-02839-y (2021).
67. Asplund, J. et al. Contrasting responses of plant and lichen carbon-based secondary compounds across an elevational gradient. *Funct. Ecol.* **35**, 330–341 (2021).
68. Wang, Y. et al. Effects of yttrium and phosphorus on growth and physiological characteristics of. *J. Rare Earths.* **36**, 781–788 (2018).
69. Maksimovic, I., Kastori, R., Putnik-Delic, M. & Borišev, M. Effect of yttrium on photosynthesis and water relations in young maize plants. *J. Rare Earths.* **32**, 372–378 (2014).
70. Białońska, D. & Dayan, F. E. Chemistry of the lichen *Hypogymnia physodes* transplanted to an industrial region. *J. Chem. Ecol.* **31**, 2975–2991 (2005).
71. Galanty, A. et al. Quantitative variations of usnic acid and selected elements in terricolous lichen Cladonia mitis Sandst, with respect to different environmental factors: A chemometric approach. *Phytochemistry* **192**, 112948 (2021).
72. Malaspina, P. et al. Bioaccumulation capacity of two chemical varieties of the lichen *Pseudevernia furfuracea*. *Ecol. Indic.* **45**, 605–610 (2014).
73. Osyczka, P., Latkowska, E. & Rola, K. Metabolic processes involved with sugar alcohol and secondary metabolite production in the hyperaccumulator lichen *Diploschistes muscorum* reveal its complex adaptation strategy against heavy-metal stress. *Fungal Biol.* **125**, 999–1008 (2021).
74. Rola, K., Latkowska, E., Ogar, W. & Osyczka, P. Towards understanding the effect of heavy metals on mycobiont physiological condition in a widespread metal-tolerant lichen *Cladonia rei*. *Chemosphere* **308**, 136365 (2022).
75. Paukov, A. et al. The effects of edaphic and climatic factors on secondary lichen chemistry: A case study using saxicolous lichens. *Diversity (Basel)* **11**, 6–11 (2019).
76. Cernava, T. et al. Plasticity of a holobiont: Desiccation induces fasting-like metabolism within the lichen microbiota. *ISME J.* **13**, 547–556 (2019).
77. Cernava, T. et al. Adaptions of lichen microbiota functioning under persistent exposure to arsenic contamination. *Front. Microbiol.* **9**, 1–12 (2018).
78. Hawksworth, D. L., Paterson, R. R. & Vote, N. An investigation into the occurrence of metabolites in obligately lichenicolous fungi from thirty genera. in *Phytochemistry and Chemotaxonomy of Lichenized Ascomycetes—A Festschrift in Honour of Siegfried Huneck* (eds. Feige, G. B. & Lumbsch, H. T.) vol. 53 101–108 (Bibliotheca Lichenologica, J. Cramer, Berlin, Germany; Stuttgart, Germany, 1993).
79. Inokoshi, J. et al. Production of a new type of amidepsine with a sugar moiety by static fermentation of *Humicola* sp. FO-2942. *J. Antibiot.* **63**, 9–16 (2010).
80. Singh, G. et al. Climate-specific biosynthetic gene clusters in populations of a lichen-forming fungus. *Environ. Microbiol.* **23**, 4260–4275 (2021).
81. Merges, D., Dal Grande, F., Valim, H., Singh, G. & Schmitt, I. Gene abundance linked to climate zone: Parallel evolution of gene content along elevation gradients in lichenized fungi. *Front. Microbiol.* **14**, 1–8 (2023).

Acknowledgements

We would like to express our gratitude to Dr. Davoud Koolivand (from the University of Zanjan, Iran) and Dr. Samaneh Chaharmiri-Dokhaharani (from Mae Fah Luang University, Thailand) for their invaluable assistance and support throughout this research endeavor. The Fondation Langlois is thanked for its supportive and financial involvement.

Author contributions

H.N and M.R.R conceived and designed the research. H.N. collected the lichen material. H.N., M.R.R., S.D., and M.O.N. conducted the experiments. H.N. and M.R.R. analyzed the data and wrote the manuscript. M.S. supervised the study, identified and vouchered the lichen samples, and revised the manuscript. J.B. supervised the work and revised the manuscript. All authors read and approved of the final manuscript. M.R.R and H.N. contributed equally to this work as first authors.

Declarations

Competing interests

The authors declare no competing interests.

Additional information

Supplementary Information The online version contains supplementary material available at https://doi.org/10.1038/s41598-025-03162-w.

Correspondence and requests for materials should be addressed to H.N.